

Preparation of YSZ solid electrolyte by slip casting and its properties

DOU Jing^{a, b}, LI Heping^a, XU Liping^a, ZHANG Lei^{a, b}, and WANG Guangwei^{a, b}

^a Laboratory for Study of the Earth's Interior and Geofluids, Institute of Geochemistry, Chinese Academy of Sciences, Guiyang 550002, China

^b Graduate School of Chinese Academy of Sciences, Beijing 100049, China

Received 19 August 2008; received in revised form 5 December 2008; accepted 10 December 2008

Abstract

Fully stabilized YSZ solid electrolyte was prepared by slip casting. The density was measured according to the Archimedes principle and the linear shrinkage was calculated from measuring the sizes of samples before and after sintering. XRD analysis was conducted to verify the phase structure of both the starting YSZ powder and the prepared YSZ electrolyte. The microstructure of fracture surface and the electrical properties of the samples sintered at different temperatures were investigated via SEM and a complex impedance method, respectively. By comparison of the properties and features among the samples, a slip casting method was established to be a simple way to manufacture high-quality YSZ electrolyte at the sintering temperature of 1550°C for 3 h, which provides a new approach for YSZ electrolyte with complex shapes and mass production.

Keywords: YSZ; solid electrolyte; slip casting; ionic conductivity

1. Introduction

Oxygen sensors with zirconia-based solid electrolytes have been widely developed. Among the zirconia-based solid electrolytes, Y_2O_3 stabilized ZrO_2 (YSZ) is one of the most used solid electrolytes in oxygen-ion conducting devices [1-2]. Under sensors' working conditions, the electrolyte plays the role of transmitting ions between electrodes. Therefore, high ionic conductivity is the basic for the application of the electrolyte.

Based on the Y_2O_3 - ZrO_2 system, a large amount of researches have been conducted [3-7]. One of the emerged common recognitions is that 8 mol%-9 mol% YSZ has the largest ionic conductivity and it is the focus of present researches. As a core component, the quality of electrolytes directly determines the quality of sensors; therefore, besides the above high ionic conductivity, solid electrolytes should have high stability, high densification, high strength, high toughness, and easy processing, etc. As a result, preparing solid electrolytes with desirable performances has become one of the hot issues.

Many methods [8-9] can be used to fabricate YSZ electrolytes. However, most are used to fabricate films. In addition, these methods have the disadvantages of using expensive devices and complex process, which greatly limits the spread and application of solid electrolytes. A slip casting

method [10] was used in this paper, and this method has the following advantages: simple technology, cheap equipment, and good ability to fabricate products with complex shape and structure [11] for preparing YSZ solid electrolytes with good performances. In this method, sintering temperature has the important influence on the densification and electrical properties of electrolytes.

2. Experimental

2.1. Sample preparation

Commercially available 8 mol% YSZ powder with a high purity and a crystallite size of 40-50 nm (Shanghai, China) was used to prepare samples. The preparation procedure of slip casting method includes slurring, grouting, shaping, sintering, etc. (see Fig. 1). In this procedure, Arabic gum was used as a dispersant and binder, and porous plaster mold as a shaping manner. 2%-3% Arabic gum (based on dry YSZ) was added to the mixed solution of water and ethanol, and intensively dissolved. Then, YSZ was added to it with efficient stirring to form a mixture of YSZ with a solid content of 50wt%. The above mixture was milled in the alumina ball milling tank for 2-3 h, followed by degassing using the vacuum technique in order to get relative stable suspension with very few bubbles. The above suspension was injected to the dry porous plaster mold continuously until

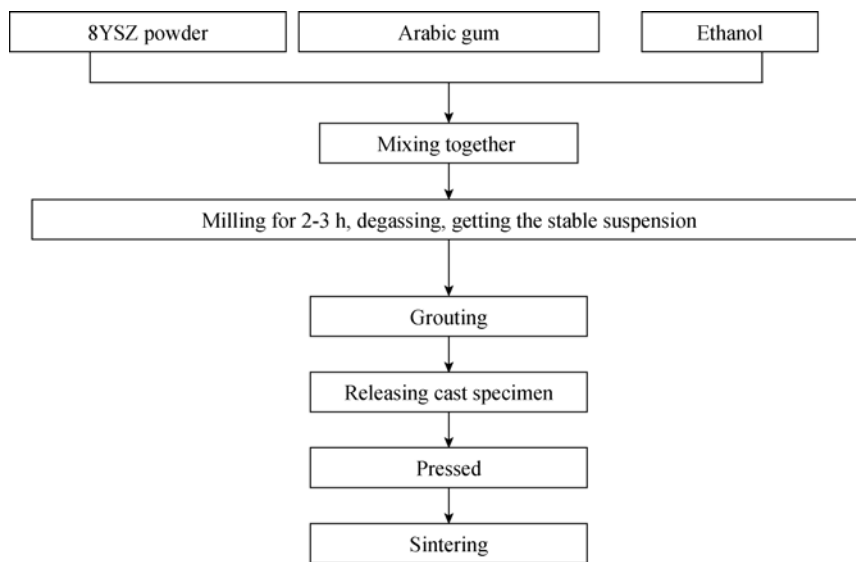


Fig. 1. Preparation procedure of YSZ by slip casting.

the liquid surface in the hole would not go down. Cast specimens were released from the mold when the plaster dried and then dried in air at 25°C for a few days. Smooth surfaces were obtained by carefully grinding off any cast protrusions. Then cast specimens were pressed under 200 MPa for about 1 min followed by being sintered in air under 1350–1550°C for 3 h and then the furnace was cooled in air.

2.2. Analyses of density, XRD, SEM, and impedance spectroscopy

Density measurements were made by the Archimedes displacement method [12]. Also, the linear shrinkage was calculated by measuring the dimensions of samples before and after sintering. X-ray diffraction (XRD) analysis using Cu K_α was conducted to verify phase structures for both the starting powder and YSZ electrolytes. The photomicrographs of fracture surfaces were observed via scanning electron microscopy (JEOL JSM-6460LV). The electrical properties of samples at different sintering temperatures were obtained by complex impedance spectroscopy (Solartron-1260 impedance/gain-phase analyzer) in air, at a frequency range of 0.1 Hz–1 MHz at temperatures of 250, 300, 350, 400, 450, 500, and 550°C. Before measuring, platinum electrodes were prepared by painting platinum paste onto both sides of the samples, and then heated at 800°C for 90 min. Z-view software was used to realize data fitting.

2.3. Nernst response

An oxygen concentration cell with YSZ solid electrolyte,

two kinds of solid buffers (Cu-Cu₂O, Ni-NiO) whose oxygen fugacities are known, and Pt electrodes, was formed. The electromotive force (emf) of the above cell was measured by the digital multimeter evaluation device (HP34401A) with the input impedance greater than 10 GΩ and it cannot introduce palpable system error in this experiment. The ion transference number was obtained through comparing the measured emf value with its corresponding theoretical one at a certain temperature.

3. Results and discussion

3.1. Microstructure

Table 1 shows that the density of samples increases as the sintering temperature increases. The density of samples sintered at 1500°C even reaches 96.4% of theoretical density [13–14]. When sintered at 1350°C, the samples have a relative density of only 88.5%. As shown in Fig. 2, from 1400°C to 1450°C, both the density and linear shrinkage of samples increase rapidly and then at a higher temperature, both increase slowly.

The fractured surfaces of the samples sintered at different sintering temperatures are shown in Fig. 3, which shows that the grain size and gas hole varied with temperature. The sintering process of YSZ is essentially the process of degassing, particle rearranging, and grain growing. Sintered at 1350°C, the samples are composed of lots of small particles and large pores (see Fig. 3(a)), although the part of them have been sintered together, there is only the point-contact

Table 1. Real density and relative density of YSZ sintered at different temperatures

Sintering temperature / °C	1350	1400	1450	1500	1550
Real density / (g·cm ⁻³)	5.273	5.374	5.636	5.744	5.756
Relative density / %	88.5	90.2	94.6	96.4	96.6

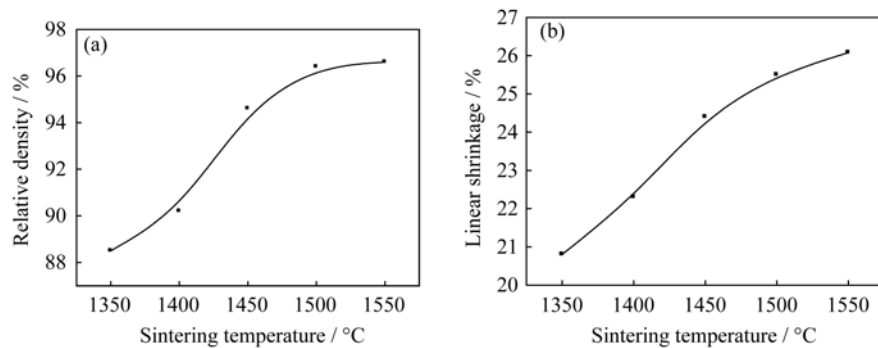


Fig. 2. Relative density (a) and linear shrinkage (b) of YSZ sintered at different temperatures.

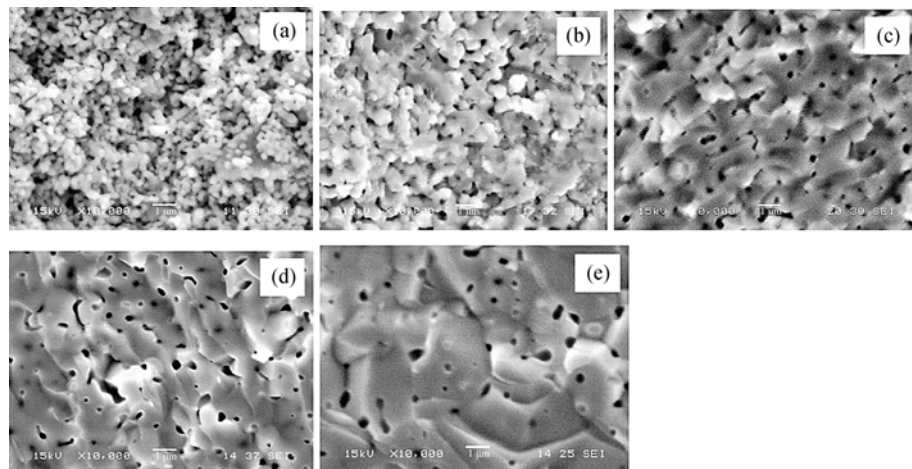


Fig. 3. SEM images of the fractured surfaces of samples sintered at different temperatures: (a) 1350°C; (b) 1400°C; (c) 1450°C; (d) 1500°C; (e) 1550°C.

among particles, which demonstrates that the sintering activity just started. Therefore, the density of samples is lower as shown in Fig. 2(a). Sintered at 1400°C (see Fig. 3(b)), it can be found that particles have significantly grown and porosity obviously reduces. During this stage, what happened was the rearrangement and bonding process of particles. When sintering temperature reached 1450°C (Fig. 3(c)), particles continuously grew, the grain boundary phase shifted to the grain junctions. The contacting area increased and large crystals formed. Pores exist in and among particles and the ones among them connected. The sintering active temperature is 1400–1450°C, during which both the density and linear shrinkage of samples increase rapidly (see Fig. 2). At a higher temperature (1500°C), as shown in Fig. 3(d), it is not found that particles grew significantly, but pores reduced and deformed, some of them disappeared. In this case, sintering driving force decreases because of the multicrystal forming. As a result, both the density and linear shrinkage of samples increased slowly (see Fig. 2). When sintered at 1550°C, porosity further reduced, and the pores deformed to isolate close holes, the density of samples improved as shown in Fig. 3(e).

X-ray diffraction analysis (Fig. 4) shows the pure cubic phase of YSZ electrolytes as well as the starting powder. This indicates that Y_2O_3 and ZrO_2 had formed a stable solid solution in the powder. Simultaneously, XRD analysis shows no change of phase structure of YSZ electrolytes in the sintering temperature range of 1350–1550°C.

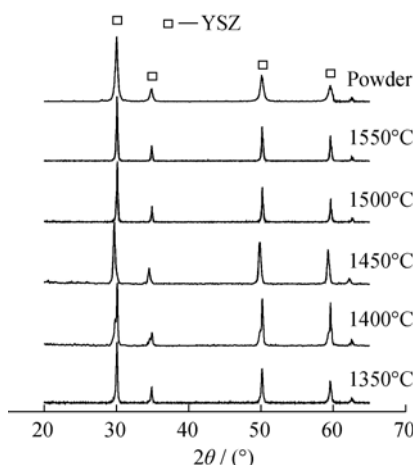


Fig. 4. XRD patterns of the YSZ sintered at different temperatures and YSZ powder.

3.2. Electrical properties

Complex impedance spectroscopy is generally accepted as a powerful tool to study the electrical properties of solid electrolytes. Fig. 5 shows the typical impedance diagram of YSZ solid electrolytes sintered at different temperatures at the operating temperature of 350°C. In the frequency range of 1 MHz-10 Hz, the two arcs represent the resistivities of grain interior and grain boundary, respectively. As shown in Fig. 5, for the samples sintered at 1350°C, the separation of the two arcs is poor, and the resistivities of both the grain interior and grain boundary are large. The reason is that the samples sintered at 1350°C have small particles (Fig. 3(a)), which lead to the high proportion of grain boundary. With the sintering temperature increasing (1450°C and 1500°C), the grains grew rapidly (see Figs. 3(c) and (d)), so the grain resistance reduces rapidly (Fig. 5). In these cases, although the area of the grain boundary reduces, the connecting pore phase among the grains greatly reduces the conductivity of the grain boundary, which is ascribed to its extremely low conductivity. Thus, the resistivity ratio of grain boundary is larger. However, from the spectroscopy of samples sintered at 1550°C, it can be found that the resistivity ratio of grain boundary is smaller than that of the grain (Fig. 5). This is due to the disappearance of the connecting pore phase existing among grains.

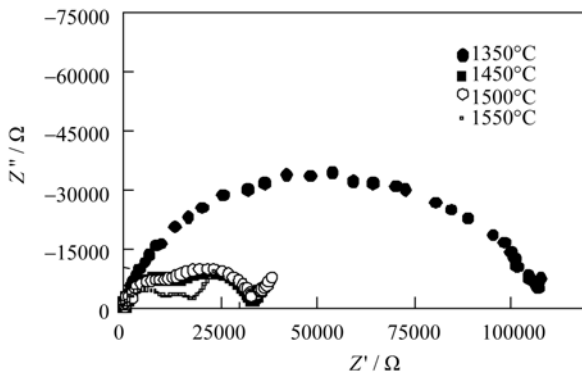


Fig. 5. Impedance diagrams of YSZ sintered at different temperatures at the operating temperature of 350°C.

The above analysis indicates that the existing pore phase has a pronounced effect on the conductivity of samples, and especially on that of grain boundary, and it can be found that impedance spectroscopy is very sensitive to the change of microstructure of solid electrolytes.

The raw impedance data allows direct resistivity plotting so the resistivity values of the grain interior and grain boundary, R_{gi} and R_{gb} , can be gotten first. The total resistivity is the sum of R_{gi} and R_{gb} , then according to $\sigma = L / SR$ (where σ is the ionic conductivity, L is the thickness of samples and S the electrode area), the ionic conductivity of the

grain interior and grain boundary, σ_{gi} and σ_{gb} , can be achieved. Then, the temperature (T) dependence of the ionic conductivity (σ) is analyzed using the Arrhenius equation: $\sigma T = \sigma_0 \exp(-E_a / kT)$.

where σ_0 is the electrical conductance, k is the Boltzmann constant, and E_a the activation energy. The temperature range for presenting impedance spectroscopy data was 300-500°C, because the two arcs are not well defined below 300°C and above 500°C.

As shown in Fig. 6, the grain interior conductivity of samples sintered at 1350°C is much lower, which originates from the small particles, as shown in Fig. 3(a); the samples sintered at 1450°C, 1500°C, and 1550°C have the close grain interior conductivity, the three curves almost coincide with each other, which indicates that the grain interior conductivity is only slightly affected by the sintering temperature. With the increase of sintering temperature, grain boundary conductivity increases at the same operating temperature (Fig. 7).

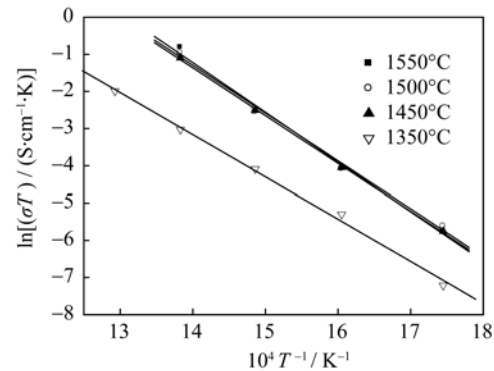


Fig. 6. Grain interior conductivities of YSZ sintered at different temperatures.

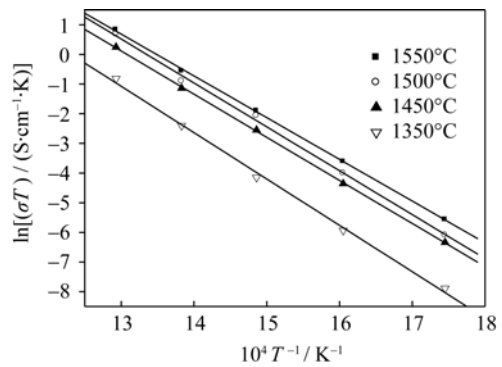


Fig. 7. Grain boundary conductivities of YSZ sintered at different temperatures.

The total conductivities of samples sintered at 1550°C are listed in Table 2. From the table, it can be found that the total conductivities increase as the operating temperature in-

creases. Below 400°C, it increases slowly, while above 400°C, it increases rapidly. At 500°C, the value is more than 10^{-3} S·cm⁻¹.

By definition, the activation energy for conduction is proportional to the Arrhenius slope. The activation energies for grain interior, grain boundary, and total conductivities

are listed in Table 3. Table 3 shows that the activation energies for grain boundary is larger than that for the grain interior; the activation energy for total conductivities of samples sintered at 1550°C is 1.17 eV, close to the reported values [15] (the activation energies for 9 mol% YSZ and 6 mol% YSZ are 1.29 eV and 1.18 eV, respectively).

Table 2. Conductivities of YSZ sintered at 1550°C

Operating temperature / °C	250	300	350	400	450	500	550
$\sigma / (\text{S}\cdot\text{cm}^{-1})$	4.50×10^{-7}	3.11×10^{-6}	1.66×10^{-5}	7.58×10^{-5}	3.45×10^{-4}	2.97×10^{-3}	1.10×10^{-2}

Table 3. Activation energy for grain interior, grain boundary and total conductivities

Sintering temperature / °C	Activation energy for conduction / eV		
	Grain interior	Grain boundary	Total
1350	0.98	1.35	1.15
1450	1.11	1.28	1.19
1500	1.11	1.26	1.19
1550	1.15	1.21	1.17

3.3. Nernst response

The oxygen concentration cell composed of YSZ solid electrolyte and two kinds of solid buffers (Cu-Cu₂O, Ni-NiO) whose oxygen fugacities are known and Pt electrode is as follows:



If the ion transference number of YSZ electrolyte is assumed to be t_{ion} ($t_{\text{ion}} \equiv \sigma_{\text{ion}} / \sigma_{\text{total}}$, where σ_{ion} is the oxygen ion conductivity, σ_{total} is the sum of oxygen ion conductivity and the electron hole conductivity), the electromotive force at both sides of YSZ solid electrolyte, E , can be represented according to the equivalent circuit of the above cell and Nernst equation

$$4EF = \int_{\mu_{\text{O}_2}^{\text{Ni-NiO}}}^{\mu_{\text{O}_2}^{\text{Cu-Cu}_2\text{O}}} t_{\text{ion}} d\mu_{\text{O}_2} \quad (1)$$

where F is the Faraday constant, μ_{O_2} is the oxygen equilibrium potential, $\mu_{\text{O}_2}^{\text{Cu-Cu}_2\text{O}}$ and $\mu_{\text{O}_2}^{\text{Ni-NiO}}$ denote the oxygen equilibrium potentials of Cu-Cu₂O and Ni-NiO, respectively. If $t_{\text{ion}} = 1$, formula (1) will be changed into the ideal Nernst equation. In this case the YSZ solid electrolyte is a pure oxygen ion conductor.

At a certain temperature, $\mu_{\text{O}_2}^{\text{Cu-Cu}_2\text{O}}$ and $\mu_{\text{O}_2}^{\text{Ni-NiO}}$ can be calculated from the μ_{O_2} - T relation formulae (2) and (3) given by O'Neill *et al.* [16-17].

$$\mu_{\text{O}_2}^{\text{Cu-Cu}_2\text{O}} = -347,705 + 246.096T - 12.9053T \ln T \quad (2)$$

$$\mu_{\text{O}_2}^{\text{Ni-NiO}} = -478,967 + 248.514T - 9.7961T \ln T \quad (3)$$

Calculated from formulae (1), (2) and (3), the theoretical emf of the above cell was 294 mV at 500°C. The samples sintered at 1550°C are taken for measuring; the measured value is 287 mV. Considering the error in the process of assembling and measuring, it can be found that YSZ solid electrolytes prepared in this paper have a good Nernst response, and the conductive mechanism is ionic conduction.

4. Conclusion

Prepared by slip casting method and sintered at 1550°C for 3 h, the YSZ electrolyte presents the advantages of having a desirable shape, better density, superior conductivity and a good Nernst response, which is totally qualified to be an intermediate-temperature solid electrolyte. Therefore, the slip casting method is a potential candidate for producing solid electrolytes with complex shapes in an inexpensive way, which allows the application of solid electrolytes to spread.

Acknowledgements

The authors wish to acknowledge the Key Laboratory of Ore Deposit Geochemistry and Chinese Academy of Sciences for help with the X-ray diffraction test; the State Key Laboratory of Environmental Geochemistry, Institute of Geochemistry, and Chinese Academy of Sciences for SEM test. This work was financially supported by the National High-Tech Research and Development Program of China (No. 2006AA09Z205), the National Natural Science Foundation of China (No. 40573046), the Science and Technology Foundation of Guizhou Province of China (No. (2006)2105) and the Large-scale Scientific Apparatus Development Program of Chinese Academy of Sciences.

References

- [1] Badwal S.P.S. and Fogar K., Solid oxide electrolyte fuel cell review, *Ceram. Int.*, 1996, **22**: 257.
- [2] Filal M., Petot C., Mokchah M., Chateau C., and Charpentier

- J.L., Ionic conductivity of yttrium-doped zirconia and the composite effect, *Solid State Ionics*, 1995, **80**: 27.
- [3] Fisher C.A.J. and Matsubara H., Oxide ion diffusion along grain boundaries in zirconia: A molecular dynamics study, *Solid State Ionics*, 1998, **113-115**: 311.
- [4] Luo J., Hairetdinov E.F., Almond D.P., and Stevens R., The characteristic frequencies for ionic conduction in 12% Y_2O_3 doped ZrO_2 , *Solid State Ionics*, 1999, **122**: 205.
- [5] Pimenov A., Ullrich J., Lunkenheimer P., Loidl A., and Rüscher C. H., Ionic conductivity and relaxations in $\text{ZrO}_2\text{-Y}_2\text{O}_3$ solid solutions, *Solid State Ionics*, 1998, **109**: 111.
- [6] Ramanmoorthy R., Sundararaman D., and Ramasamy S., Ionic conductivity studies of ultrafine-grained yttria stabilized zirconia polymorphs, *Solid State Ionics*, 1999, **123**: 271.
- [7] Sawaguchi N. and Ogawa H., Stimulated diffusion of oxide ions in $\text{YO}_{1.5}\text{-ZrO}_2$ at high temperature, *Solid State Ionics*, 2000, **128**: 183.
- [8] Kitagawa N. and Kitoh M., *Solid Oxide Fuel Cell and Method of Manufacturing the Same*, US Patent, US5051321, 1991.
- [9] Minh N.Q. and Horne C.R., *Apparatus and Method of Fabricating a Monolithic Solid Oxide Fuel Cell*, US Patent, US5162167, 1992.
- [10] He T.M., Pei L., Lü Z., Liu J., and Su W.H., Preparation of tubular YSZ electrolyte and its application in solid oxide fuel cells, *J. Functional Mater.* (in Chinese), 2001, **32** (1): 55.
- [11] He T.M., Lü Z., Huang Y.L., Guan P.F., Huang X.Q., Liu Z.G., Pei L., Su W.H., Study on preparation and properties of YSZ electrolyte membrane tubes with low cost, *J. Funct. Mater.* (in Chinese), 2002, **33** (1): 70.
- [12] Zhu G.H., *Technique Experiment for Ceramic* (in Chinese), China Construction Industry Press, Beijing, 1987: 48.
- [13] Xin X.S., Lü Z., Huang X.Q., Sha X.Q., Zhang Y.H., and Su W.H., Influence of synthesis routes on the performance from weakly agglomerated yttria-stabilized zirconia nanomaterials, *Mater. Res. Bull.*, 2006, **41** (7): 1319.
- [14] Wang Z.C., Davies T.J., and Ridley N., Net shape fabrication of ceramic specimens for superplastic tensile testing. *Scripta Metall. Mater.*, 1993, **28** (3): 301.
- [15] Somiya S., Yamamoto N., and Yanagda H., *Science and Technology of Zirconia III*, the American Ceramic Society, Westerville, 1988: 837.
- [16] O'Neill H.St.C., System Fe-O and Cu-O: Thermodynamic data for the equilibria Fe-FeO , $\text{Fe-Fe}_3\text{O}_4$, $\text{FeO-Fe}_3\text{O}_4$, $\text{Fe}_3\text{O}_4\text{-Fe}_2\text{O}_3$, $\text{Cu-Cu}_2\text{O}$, and $\text{Cu}_2\text{O-CuO}$ from emf measurements, *Am. Miner.*, 1988, **73**: 470.
- [17] O'Neill H.St.C. and Pownceby M.I., Thermodynamic data from redox reaction at high temperatures: I. An experimental and theoretical assessment of the electrochemical method using stabilized zirconia electrolytes, with revised values for the Fe-FeO , Co-CoO , Ni-NiO and $\text{Cu-Cu}_2\text{O}$ oxygen buffers, and new data for the W-WO_2 buffer. *Contrib. Mineral. Petrol.*, 1993, **114**: 296.